

## Heterogeneous Nucleation in Finite-Size Adaptive Dynamical Networks

Jan Fialkowski<sup>1,\*</sup>, Serhiy Yanchuk<sup>2,3</sup>, Igor M. Sokolov<sup>4,5</sup>, Eckehard Schöll<sup>1,2,6</sup>,  
Georg A. Gottwald<sup>7</sup>, and Rico Berner<sup>1,4,†</sup>

<sup>1</sup>*Institute for Theoretical Physics, Technische Universität Berlin, Hardenbergstraße 36, 10623 Berlin, Germany*

<sup>2</sup>*Potsdam Institute for Climate Impact Research, Telegrafenberg A 31, 14473 Potsdam, Germany*

<sup>3</sup>*Institute of Mathematics, Humboldt-Universität zu Berlin, 12489 Berlin, Germany*

<sup>4</sup>*Department of Physics, Humboldt-Universität zu Berlin, Newtonstraße 15, 12489 Berlin, Germany*

<sup>5</sup>*IRIS Adlershof, Humboldt-Universität zu Berlin, Zum Großen Windkanal 6, 12489 Berlin, Germany*

<sup>6</sup>*Bernstein Center for Computational Neuroscience Berlin, Humboldt-Universität zu Berlin, 10115 Berlin, Germany*

<sup>7</sup>*School of Mathematics and Statistics, University of Sydney, Camperdown New South Wales 2006, Australia*

 (Received 5 July 2022; revised 17 October 2022; accepted 10 January 2023; published 10 February 2023)

Phase transitions in equilibrium and nonequilibrium systems play a major role in the natural sciences. In dynamical networks, phase transitions organize qualitative changes in the collective behavior of coupled dynamical units. Adaptive dynamical networks feature a connectivity structure that changes over time, coevolving with the nodes' dynamical state. In this Letter, we show the emergence of two distinct first-order nonequilibrium phase transitions in a finite-size adaptive network of heterogeneous phase oscillators. Depending on the nature of defects in the internal frequency distribution, we observe either an abrupt single-step transition to full synchronization or a more gradual multistep transition. This observation has a striking resemblance to heterogeneous nucleation. We develop a mean-field approach to study the interplay between adaptivity and nodal heterogeneity and describe the dynamics of multicluster states and their role in determining the character of the phase transition. Our work provides a theoretical framework for studying the interplay between adaptivity and nodal heterogeneity.

DOI: [10.1103/PhysRevLett.130.067402](https://doi.org/10.1103/PhysRevLett.130.067402)

Phase transitions play an important role in the natural sciences [1]. Complex dynamical networks [2,3] exhibit a plethora of nonequilibrium phase transitions organizing their collective dynamics in response to variations in control parameters such as interaction strength or noise [4,5]. In particular, transitions between coherence and incoherence have attracted significant attention in static [6] and temporally evolving complex networks [7]. The Kuramoto model [8] has served as a test bed to study phase transitions in networks of coupled oscillators. It exhibits either first or second-order phase transitions from incoherence to full synchronization, depending on the natural frequency distribution [8–13]. Similarly, network structure [14] and weight distribution [15] can lead to first-order (or explosive) transitions and to hysteresis, for which a universal mechanism has recently been proposed [16].

To better describe real-world phenomena, the original Kuramoto model has been extended and modified. Beyond the classical Kuramoto model, generalizations to static and time-evolving networks have been developed [7,17–22]. The inclusion of additional dynamical degrees of freedom, e.g., to describe power grids [23–27] by including inertia, has introduced much richer synchronization transitions with regimes of coexisting cluster states. Recently, adaptive dynamical network models were introduced which are capable of describing chemical [28,29], epidemic [30],

biological [31], neurological [32–34], transport [35], and social systems [36,37]. Adaptive dynamical networks are characterized by the coevolution of network structure and functionality. Paradigmatic models of adaptively coupled phase oscillators have recently attracted much attention [38–43]. They have shown promise in predicting and describing phenomena in more realistic and complex physical systems such as neuronal and biological systems [44–47], as well as power grid models [48]. However, the type and nature of phase transition in this important class of models remains unclear.

This work characterizes nonequilibrium phase transitions in adaptive networks. We describe phase transitions in a finite-size Kuramoto model equipped with adaptive coupling weights. The natural frequencies are considered to be uniformly distributed, i.e., all possible frequencies are equally probable, and therefore disorders induced by finite-size realizations of this distribution impact directly the synchronization behavior. We find two qualitatively distinct types of first-order transitions to synchrony akin to first-order transition phenomena of heterogeneous nucleation [49]. The first, *multistep* type of synchronization transition is characterized by the nucleation and growth of a dominant cluster, similar to Ostwald ripening in equilibrium and nonequilibrium systems [50], until the system reaches synchrony. The second, *single-step* transition type features

multiple stable synchronization nuclei, and the transition to full synchrony is caused by an abrupt merging of large clusters of similar size. These two paths to synchrony exhibit a high degree of multistability. We identify the location of fluctuations in the realization of the natural frequency distribution as the cause for the two different scenarios. Methodologically, we present a framework reducing high-dimensional adaptive networks to a few mesoscopic variables and show that a collection of partially synchronized clusters of approximately equal size is more stable against changes in the coupling strength. With this, we extend the scope of mean-field approaches beyond the static network paradigm to adaptive networks.

For neuronal systems with spike-timing-dependent synaptic plasticity, phase oscillator models with phase difference-dependent adaptation functions have been introduced to explain effects stemming from long-term potentiation and depression [39,44,45,51,52]. Beyond that, phase oscillator models have served as paradigms for studying collective behavior in real-world dynamical systems [53]. We consider the adaptively coupled phase oscillator model

$$\frac{d\phi_i}{dt} = \omega_i - \frac{\sigma}{N} \sum_{j=1}^N \kappa_{ij} \sin(\phi_i - \phi_j), \quad (1)$$

$$\frac{d\kappa_{ij}}{dt} = -\epsilon[\kappa_{ij} + \sin(\phi_i - \phi_j + \beta)], \quad (2)$$

for  $N$  phase oscillators  $i = 1, \dots, N$  with phases  $\phi_i(t) \in [0, 2\pi)$  coevolving with adaptive coupling weights  $\kappa_{ij}(t)$ . The natural frequency  $\omega_i$  of the  $i$ th oscillator is drawn randomly from a uniform distribution  $\omega_i \in [-\hat{\omega}, \hat{\omega}]$  [54]. The overall coupling strength is  $\sigma$ , and  $\epsilon$  characterizes the timescale separation between the fast oscillator dynamics and the slower adaptation of the coupling weights. The parameter  $\beta$  accounts for different adaptation rules, e.g., a causal rule ( $\beta = 0$ ) or a symmetric rule ( $\beta = -\pi/2$ ) where the order of the phases or their closeness determines the sign of the coupling weight change [51,55]. Here we focus on symmetric adaptation rules which support synchronization [39]; see [56] for other adaptation rules.

Coherence can be quantified by the synchronization index  $S$  which measures the fraction of frequency-synchronized oscillator pairs  $S := (1/N^2) \sum_{i,j=1}^N s_{ij}$ , where  $s_{ij} = 1$  for equal mean phase velocities of the oscillators  $i$  and  $j$ ,  $\langle \dot{\phi}_i \rangle = \langle \dot{\phi}_j \rangle$ , and  $s_{ij} = 0$  otherwise [57]. Here  $\langle x \rangle = \lim_{T \rightarrow \infty} (1/T) \int_{T_0}^{T_0+T} x(t) dt$  with sufficiently large transient time  $T_0$ . For  $S = 1$  the system is fully frequency-synchronized, whereas for  $S = 0$  the system is asynchronous.

With increasing coupling strength  $\sigma$ , system (1)–(2) undergoes a transition from asynchrony to full synchronization, see Fig. 1(a) and Supplemental Material [56]. The routes to synchrony with increasing coupling strength  $\sigma$  in

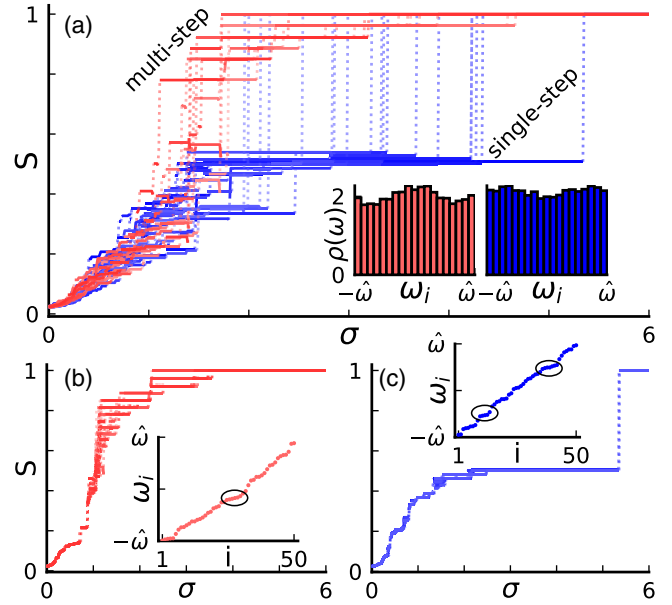


FIG. 1. Paths to synchrony for system (1)–(2). (a) Synchronization index  $S$  as a function of the coupling strength  $\sigma$  for 100 simulations with  $N = 50$  oscillators. Each run was initiated with random initial conditions and  $\sigma$  was increased in steps of  $\Delta\sigma = 0.01$ . For details on the up-sweep protocol, we refer to [56]. For each run, natural frequencies are drawn independently from a uniform distribution  $\omega_i \in [-\hat{\omega}, \hat{\omega}]$  with  $\hat{\omega} = 0.25$ . The dotted lines indicate jumps in the synchronization index during the transition. The inset shows realizations of the finite-size frequency distributions for the multistep (left) and single-step (right) paths generated from 1000 simulations. (b),(c) Synchronization index  $S$  for fixed realization of the natural frequencies and 30 different initial conditions, consistently leading to the multistep (b) or single-step transition (c). Insets show the natural frequencies used in the simulations. The circles highlight areas of higher frequency densities. The synchronization index  $S$  is determined with an averaging time window  $T = 7 \times 10^3$  and transient time  $T_0 = 3 \times 10^3$ . Other parameters:  $\beta = -0.53\pi$ ,  $\epsilon = 0.01$ .

Fig. 1(a) follow two paths of first-order transitions: a gradual multistep (upper, red) and an abrupt single-step (lower, blue) path featuring multiple small steps or a single large step in the transition to synchrony, respectively. In what follows, we describe these paths and determine the finite-size features in the realization of the natural frequency distribution that lead to either a multistep or single-step transition to synchrony.

Figures 1(b) and 1(c) show the multistep and single-step transitions, respectively, for two representative realizations of the natural frequencies (displayed as insets) and 30 different initial conditions of the phases  $\phi_i(0)$ . Depending on initial conditions and natural frequencies the system can develop a large number of coexisting states. The multistep path in Fig. 1(b) exhibits a higher degree of multistability even for the fixed realization of frequencies and a large number of transitions between coexisting states. Figures 2(a)–2(d) show snapshots of the

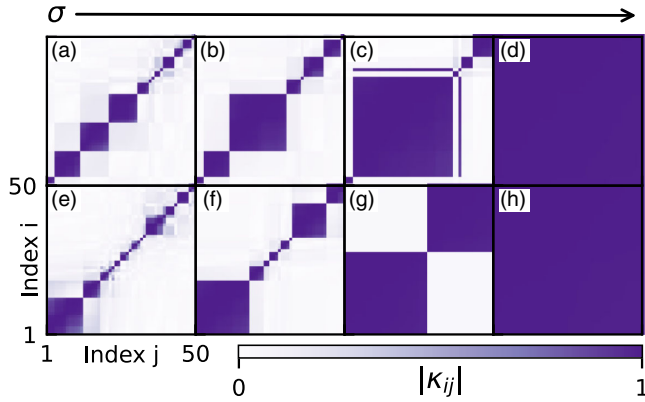


FIG. 2. Coupling matrices for specific values of  $\sigma$ , corresponding to two different types of synchronization transition. (a)–(d) multistep, and (e)–(h) single-step transition. The values of  $\sigma$  are (a) 0.9, (b) 1.05, (c) 1.75, (d) 6.0, and (e) 0.55, (f) 1.75 (g) 2.75, and (h) 6.0. The snapshots are taken after  $10^4$  time units. Other parameters:  $\hat{\omega} = 0.25$ ,  $\beta = -0.53\pi$ , and  $\epsilon = 0.01$ . Because of the  $\phi \rightarrow \phi + \pi$  symmetry,  $\kappa_{ij}$  and  $-\kappa_{ij}$  are indistinguishable, therefore the absolute values  $|\kappa_{ij}|$  are plotted, see [56].

coupling matrix corresponding to the multistep transition. It is seen that a cluster nucleus emerges and, upon increasing the coupling strength, entrains more and more oscillators leading to the fully frequency synchronized state in Fig. 2(d), similarly as observed in [23]. Depending on the initial conditions the exact structure of the system's state can vary, e.g., the size of the nucleus for different  $\sigma$ . This gives rise to a multitude of stable states for most values of  $\sigma$ .

The single-step transition is shown in Fig. 1(c). Regardless of the initial condition, the dynamics follows very similar paths of the synchronization index. The phase oscillators organize into a small number of clusters within each of which all oscillators move with the same mean phase velocity for small values of  $\sigma$ . Notably, there is no single cluster at any time that is significantly larger than the others, in contrast to the multistep transition and prior findings for multicluster states [40]. Further, for the single-step phase transition path an intermediate state with  $S \approx 0.5$  emerges, which is stable for a wide range of coupling strengths  $\sigma$ . The transition to full frequency synchronization occurs discontinuously at  $\sigma \approx 5.35$ . The formation of small initial clusters and the intermediate state are shown in Figs. 2(e)–2(h). The intermediate state (g) consists of two almost evenly sized clusters (nuclei) that are formed simultaneously.

Whether the system undergoes a multistep or a single-step transition path is determined by the particular realization of the natural frequency distribution, see the insets in Fig 1(a). Frequency distributions corresponding to multistep phase transitions are characterized by a higher density around the average frequency  $\bar{\omega} = 0$ , leading to an initial cluster with average cluster frequency close to the overall

average frequency of the network. On the other hand, frequency distributions corresponding to single-step transitions are characterized by deviations which are concentrated away from the average frequency. This leads to local clusters emerging at low coupling strength around those seeds. These clusters survive a further increase in coupling strength entraining further oscillators before, for larger coupling strength, collapsing into the fully synchronized state.

The distinction between these two qualitatively very different scenarios of phase transitions is hence caused by finite-size-induced inhomogeneities of the natural frequency distribution. The fluctuations in the realization of the natural frequencies are much more influential than the choice of initial conditions, see Figs. 1(b) and 1(c). To further probe that the choice of transition path is indeed a finite-size effect, we choose equidistantly distributed frequencies, to remove fluctuations. In this case the transition path which is taken by the system is determined instead by the initial condition of the phases, see [56].

Performing a down-sweep from large  $\sigma$  for the given frequency distributions in Figs. 1(b) and 1(c), hysteresis and bistability between full and partial cluster synchrony is observed, see [56].

During the transition to synchrony, oscillators group into phase-locked clusters. The fluctuations in the realization of the natural frequencies determine the shapes of the emerging cluster states which in turn govern the type of transition. In systems with adaptive coupling weights there are many ways in which an arbitrary number of oscillators can form a multicluster structure [40,58]. In the following, we study the coexistence of multicluster states and show that states with equally sized clusters are stable for a larger interval in  $\sigma$  than states with strongly different cluster sizes. For this, we develop a mean-field description of multiclusters employing the collective coordinate method introduced in [59]. The latter has been successfully used to describe the synchronization of the Kuramoto system for general frequency distributions [60], complex coupling topologies [61] and chaotic cluster dynamics [60]. This approach can capture finite-size effects while still reproducing the findings of mean-field theories [62].

Following [60], we assign each oscillator to one of  $M$  clusters  $\mu$  of size  $N_\mu = n_\mu N$ . The phase variables and coupling variables are written as

$$\phi_i(t) \approx \hat{\phi}_i^\mu(t) = \vartheta_\mu(t)(\omega_i - \Omega_\mu) + f_\mu(t), \quad (3)$$

$$\kappa_{ij}(t) \approx \hat{\kappa}_{ij}^{\mu\nu}(t) = \kappa_{\mu\nu}(t). \quad (4)$$

In this ansatz each phase oscillator is parametrized by  $\vartheta_\mu(t)$  describing the spread within the  $\mu$ th cluster with relative frequencies  $(\omega_i - \Omega_\mu)$ , where  $\Omega_\mu = N_\mu^{-1} \sum_{i \in \mathcal{C}_\mu} \omega_i$  is the mean natural frequency of cluster  $\mu$  with index set  $\mathcal{C}_\mu$ , and the collective phase  $f_\mu(t)$  of each respective cluster. The coupling weights  $\kappa_{ij}$  are assumed to be constant within each

cluster and only vary across clusters. Our ansatz (1)–(2) changes the microscopic description  $(\phi_i, \kappa_{ij})$  to a mesoscopic description for the clusters with the new collective coordinates  $\vartheta_\mu$ ,  $f_\mu$ , and  $x_{\mu\nu}$  [63]. This reduces the high-dimensional system (1)–(2) from  $N + N^2$  to  $2M - 1 + M^2$  dimensions.

The equations of motion for the collective coordinates are obtained by minimizing the error made by the assumption (3)–(4), see [56,59,62] for details. For simplicity, we restrict ourselves in the following to the description of two clusters in the continuum limit  $N \rightarrow \infty$  with fixed size ratios  $n_1$  and  $n_2 = 1 - n_1$  [64]. We introduce the order parameter for each cluster  $r_\mu = (1/N) |\sum_{j \in C_\mu} e^{i\phi_j^t}|$  that in the continuum limit is approximated by  $r_\mu = \sin z/z$  with  $z = \vartheta_\mu n_\mu/4$  [8,59]. The resulting mesoscopic dynamics of system (1)–(2) is governed by

$$\dot{\vartheta}_\mu = 1 + \frac{48\sigma}{n_\mu^2 \vartheta_\mu} \left[ \cos\left(\frac{\vartheta_\mu n_\mu}{4}\right) - r_\mu \right] \times [x_{\mu\mu} n_\mu r_\mu + x_{\mu\nu} n_\nu r_\nu \cos f], \quad (5a)$$

$$\dot{f} = -\frac{1}{4} - \sigma r_1 r_2 (n_1 x_{21} + n_2 x_{12}) \sin f, \quad (5b)$$

$$\dot{x}_{\mu\nu} = -\epsilon [x_{\mu\nu} + r_\mu r_\nu \sin(f_\mu - f_\nu + \beta)], \quad (5c)$$

with  $\mu, \nu \in \{1, 2\}$ ,  $f = f_1 - f_2$  is the phase difference of the two clusters. See [56] for details.

Figure 3 shows a comparison of the high-dimensional adaptive Kuramoto system (1)–(2) and the reduced system (5). We use  $N = 1000$  oscillators with a fixed realization of natural frequencies to probe the continuum limit ( $N \rightarrow \infty$ ) mean-field approach. For two-cluster configurations with a varying relative number of oscillators in the first cluster from  $n_1 = 0.5$  to  $n_1 = 0.95$ , we prepare special initial conditions that result in the desired state, see [56]. For the reduced system, we proceed analogously.

Figure 3 shows that the dynamics of the two-cluster state is captured fully by the collective coordinate framework. The solid lines (full system) overlap with the dashed lines (reduced system). The single-step transition, also seen in Fig. 1(c), is well explained by the merging of two clusters in the reduced system. In both systems the multicluster structure ceases to exist beyond a certain coupling strength  $\sigma_c$ . The critical values for the onset of cluster  $\sigma_c$  and full synchronization  $\sigma_s$  are well approximated by a perturbative approach for  $\epsilon \ll 1$  to the reduced system (5). We obtain  $\sigma_c \approx 0.460$  and  $\sigma_s \approx 3.152$ , see [56]. In particular, the analytic result shows that multicluster states exist only for an intermediate range of  $\sigma$ , which agrees with the observations in Fig. 1.

In the inset of Fig. 3 the excellent agreement between the oscillator phases of the full system and the collective coordinate ansatz (3) is shown for  $n_1 = 0.5$ .

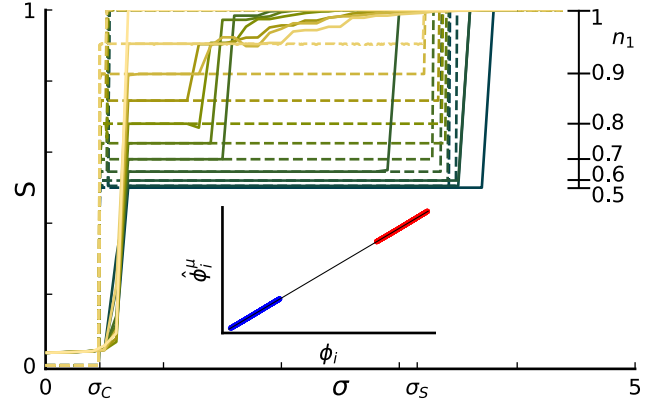


FIG. 3. Bifurcation diagram for the adaptive Kuramoto model (1)–(2) (full system) with  $N = 1000$  oscillators (solid lines) and the reduced system (5) (dashed lines), showing the synchronization index  $S$  as a function of the coupling strength  $\sigma$ . For the full system a two-cluster state is initially prepared with a fraction of  $n_1$  oscillators placed in the first cluster, and  $n_2 = 1 - n_1$  oscillators in the second cluster at  $\sigma = 1$ , for the reduced system at  $\sigma = 0.5$  with values of  $n_1$  from 0.5 to 0.95 in steps of  $\Delta n_1 = 0.05$ . Additionally the full system is simulated for  $n_1 = 1$  to visualize hysteresis. The analytical estimates of upper and lower bounds of two-cluster existence at  $\sigma_s = 3.152$  and  $\sigma_c = 0.460$  are marked on the axis. Inset: oscillator phases  $\phi_i$  for the full system vs the approximation  $\hat{\phi}_i^\mu = \vartheta_\mu \omega_i$  of the reduced system for  $n_1 = 0.5$  and  $\sigma = 2$ ; colors denote the two clusters. Other parameters:  $\hat{\omega} = 0.25$ ,  $\beta = -0.53\pi$ , and  $\epsilon = 0.01$ .

Figure 3 shows that two-cluster states in the reduced system are stable for a much larger interval in  $\sigma$  than in the full system. This discrepancy may be linked to the observation that the stability of multicluster states is mainly determined by intracluster links [65]. Such intracluster effects are not captured by our mean-field ansatz. However, the reduced system provides important insights into the existence of partially synchronized clusters from which the stability can be studied numerically employing the full system. This is relevant to the two transition scenarios observed in Fig. 1: for the reduced two-cluster system the values for which full synchronization emerges are larger the more equal the respective cluster sizes are with a maximum at  $n_1 = n_2 = 0.5$ . Hence a homogeneous collection of clusters of similar size will remain stable for a wide range of coupling strengths whereas heterogeneous nucleation with a dominant initial cluster will entrain further oscillators upon increasing the coupling strength.

In summary, we have shown two qualitatively different transitions to synchronization induced by the interplay of an adaptive network structure and finite-size inhomogeneities in the natural frequency distributions: single-step and multistep transitions. The transition through multiclusters makes these two phenomena different to explosive synchronization reported for systems with single or multiple adaptive coupling weights [66–68]. In the multistep transition, a single large cluster (nucleus) forms around an

inhomogeneity in the frequency distribution and successively grows until full synchronization is reached. In contrast, in the single-step synchronization transition, multiple equally sized clusters (nuclei) form around multiple inhomogeneities, grow, and coexist stably. Each cluster moves with its mean frequency, which results in a higher difference of the average phase velocity between the clusters than between two freely moving oscillators. This higher difference inhibits the synchronization of the clusters for a significant range in the coupling strengths. Hence, this explains the observed abrupt first-order transition to full synchronization for high coupling strengths.

The described nucleation phenomena are very similar to heterogeneous nucleation induced by local impurities known, e.g., from cloud formation [69], crystal growth [70], or Ostwald ripening in equilibrium and nonequilibrium systems [50]. Because of this relation, our results provide an intriguing bridge between synchronization transitions in finite-size dynamical complex networks and thermodynamic phase transitions where the finite-size induced inhomogeneities in the natural frequencies take the role of impurities. Our numerical investigation has been complemented by a mean-field theory capable of describing multicluster states in the presence of an arbitrary frequency distribution and adaptive coupling weights. By this, we contribute to the research on mean-field models of coupled phase oscillators [71] where only recently first steps have been undertaken to include adaptive coupling [72]. Remarkably, our reduced mean-field model provides an excellent approximation of the macroscopic multicluster dynamics as well as the microscopic phase relations. The multistep transition, with a continually changing size of the main cluster (nucleus) and the importance of the stability of each cluster, is only partially captured by the mean-field approach introduced in this work. This limitation, however, could be overcome by generalizing methods on partial synchronization in generalized Kuramoto systems [23,62,73,74].

S. Y., E. S. and R. B. acknowledge funding from the German Research Foundation (DFG) under Project No. 440145547. S. Y. acknowledges funding from the DFG under Project No. 411803875. G. A. G. acknowledges support from the Australian Research Council under Grant No. DP180101991.

---

\*jan.fialkowski@campus.tu-berlin.de  
†rico.berner@physik.hu-berlin.de

- [1] H. E. Stanley, *Phase Transitions and Critical Phenomena* (Clarendon Press, Oxford, 1971).
- [2] M. E. J. Newman, The structure and function of complex networks, *SIAM Rev.* **45**, 167 (2003).
- [3] S. Boccaletti, A. N. Pisarchik, C. I. del Genio, and A. Amann, *Synchronization: From Coupled Systems to*

*Complex Networks* (Cambridge University Press, Cambridge, England, 2018).

- [4] H. Haken, *Synergetics, An Introduction*, 3rd ed. (Springer, Berlin, 1983).
- [5] E. Schöll, *Nonequilibrium Phase Transitions in Semiconductors* (Springer, Berlin, 1987).
- [6] F. A. Rodrigues, T. K. D. M. Peron, P. Ji, and J. Kurths, The Kuramoto model in complex networks, *Phys. Rep.* **610**, 1 (2016).
- [7] D. Ghosh, M. Frasca, A. Rizzo, S. Majhi, S. Rakshit, K. Alfaro-Bittner, and S. Boccaletti, The synchronized dynamics of time-varying networks, *Phys. Rep.* **949**, 1 (2022).
- [8] Y. Kuramoto, *Chemical Oscillations, Waves and Turbulence* (Springer-Verlag, Berlin, 1984).
- [9] A. Pikovsky, M. Rosenblum, and J. Kurths, *Synchronization: A Universal Concept in Nonlinear Sciences*, 1st ed. (Cambridge University Press, Cambridge, England, 2001).
- [10] D. Pazó, Thermodynamic limit of the first-order phase transition in the Kuramoto model, *Phys. Rev. E* **72**, 046211 (2005).
- [11] J. Gómez-Gardeñes, S. Gómez, A. Arenas, and Y. Moreno, Explosive Synchronization Transitions in Scale-Free Networks, *Phys. Rev. Lett.* **106**, 128701 (2011).
- [12] S. Boccaletti, J. A. Almendral, S. Guan, I. Leyva, Z. Liu, I. Sendiña-Nadal, Z. Wang, and Y. Zou, Explosive transitions in complex networks' structure and dynamics: Percolation and synchronization, *Phys. Rep.* **660**, 1 (2016).
- [13] R. M. D'Souza, J. Gómez-Gardeñes, J. Nagler, and A. Arenas, Explosive phenomena in complex networks, *Adv. Phys.* **68**, 123 (2019).
- [14] J. Gómez-Gardeñes, Y. Moreno, and A. Arenas, Paths to Synchronization on Complex Networks, *Phys. Rev. Lett.* **98**, 034101 (2007).
- [15] X. Zhang, X. Hu, J. Kurths, and Z. Liu, Explosive synchronization in a general complex network, *Phys. Rev. E* **88**, 010802(R) (2013).
- [16] C. Kuehn and C. Bick, A universal route to explosive phenomena, *Sci. Adv.* **7**, eabe3824 (2021).
- [17] M. K. S. Yeung and S. H. Strogatz, Time Delay in the Kuramoto Model of Coupled Oscillators, *Phys. Rev. Lett.* **82**, 648 (1999).
- [18] S. H. Strogatz, From Kuramoto to Crawford: Exploring the onset of synchronization in populations of coupled oscillators, *Physica (Amsterdam)* **143D**, 1 (2000).
- [19] W. S. Lee, E. Ott, and T. M. Antonsen, Large Coupled Oscillator Systems with Heterogeneous Interaction Delays, *Phys. Rev. Lett.* **103**, 044101 (2009).
- [20] M. Breakspear, S. Heitmann, and A. Daffertshofer, Generative models of cortical oscillations: Neurobiological implications of the Kuramoto model, *Front. Hum. Neurosci.* **4**, 190 (2010).
- [21] A. Nabi and J. Moehlis, Single input optimal control for globally coupled neuron networks, *J. Neural Eng.* **8**, 065008 (2011).
- [22] C. Bick, M. Goodfellow, C. R. Laing, and E. A. Martens, Understanding the dynamics of biological and neural oscillator networks through exact mean-field reductions: A review, *J. Math. Neurosci.* **10**, 9 (2020).
- [23] S. Olmi, A. Navas, S. Boccaletti, and A. Torcini, Hysteretic transitions in the Kuramoto model with inertia, *Phys. Rev. E* **90**, 042905 (2014).

- [24] L. Tumash, S. Olmi, and E. Schöll, Effect of disorder and noise in shaping the dynamics of power grids, *Europhys. Lett.* **123**, 20001 (2018).
- [25] L. Tumash, S. Olmi, and E. Schöll, Stability and control of power grids with diluted network topology, *Chaos* **29**, 123105 (2019).
- [26] H. Taher, S. Olmi, and E. Schöll, Enhancing power grid synchronization and stability through time delayed feedback control, *Phys. Rev. E* **100**, 062306 (2019).
- [27] F. Hellmann, P. Schultz, P. Jaros, R. Levchenko, T. Kapitaniak, J. Kurths, and Y. Maistrenko, Network-induced multistability through lossy coupling and exotic solitary states, *Nat. Commun.* **11**, 592 (2020).
- [28] S. Jain and S. Krishna, A model for the emergence of cooperation, interdependence, and structure in evolving networks, *Proc. Natl. Acad. Sci. U.S.A.* **98**, 543 (2001).
- [29] C. Kuehn, Multiscale dynamics of an adaptive catalytic network, *Math. Model. Nat. Phenom.* **14**, 402 (2019).
- [30] T. Gross, C.J.D. D’Lima, and B. Blasius, Epidemic Dynamics on an Adaptive Network, *Phys. Rev. Lett.* **96**, 208701 (2006).
- [31] S.R. Proulx, D.E.L. Promislow, and P.C. Phillips, Network thinking in ecology and evolution, *Trends Ecol. Evol.* **20**, 345 (2005).
- [32] W. Gerstner, R. Kempter, J.L. von Hemmen, and H. Wagner, A neuronal learning rule for sub-millisecond temporal coding, *Nature (London)* **383**, 76 (1996).
- [33] C. Meisel and T. Gross, Adaptive self-organization in a realistic neural network model, *Phys. Rev. E* **80**, 061917 (2009).
- [34] K. Mikkelsen, A. Imparato, and A. Torcini, Emergence of Slow Collective Oscillations in Neural Networks with Spike-Timing Dependent Plasticity, *Phys. Rev. Lett.* **110**, 208101 (2013).
- [35] E. A. Martens and K. Klemm, Transitions from trees to cycles in adaptive flow networks, *Front. Phys.* **5**, 62 (2017).
- [36] T. Gross and B. Blasius, Adaptive coevolutionary networks: A review, *J. R. Soc. Interface* **5**, 259 (2008).
- [37] L. Horstmeyer and C. Kuehn, Adaptive voter model on simplicial complexes, *Phys. Rev. E* **101**, 022305 (2020).
- [38] R. Gutiérrez, A. Amann, S. Assenza, J. Gómez-Gardeñes, V. Latora, and S. Boccaletti, Emerging Meso- and Macroscales from Synchronization of Adaptive Networks, *Phys. Rev. Lett.* **107**, 234103 (2011).
- [39] D. V. Kasatkin, S. Yanchuk, E. Schöll, and V. I. Nekorkin, Self-organized emergence of multi-layer structure and chimera states in dynamical networks with adaptive couplings, *Phys. Rev. E* **96**, 062211 (2017).
- [40] R. Berner, E. Schöll, and S. Yanchuk, Multiclusters in networks of adaptively coupled phase oscillators, *SIAM J. Appl. Dyn. Syst.* **18**, 2227 (2019).
- [41] R. Berner, J. Sawicki, and E. Schöll, Birth and Stabilization of Phase Clusters by Multiplexing of Adaptive Networks, *Phys. Rev. Lett.* **124**, 088301 (2020).
- [42] P. Feketa, A. Schaum, and T. Meurer, Synchronization and multi-cluster capabilities of oscillatory networks with adaptive coupling, *IEEE Trans. Autom. Control* **66**, 3084 (2020).
- [43] R. Berner, S. Vock, E. Schöll, and S. Yanchuk, Desynchronization Transitions in Adaptive Networks, *Phys. Rev. Lett.* **126**, 028301 (2021).
- [44] L. Lücken, O. V. Popovych, P. A. Tass, and S. Yanchuk, Noise-enhanced coupling between two oscillators with long-term plasticity, *Phys. Rev. E* **93**, 032210 (2016).
- [45] V. Röhr, R. Berner, E. L. Lameu, O. V. Popovych, and S. Yanchuk, Frequency cluster formation and slow oscillations in neural populations with plasticity, *PLoS One* **14**, e0225094 (2019).
- [46] J. Sawicki, R. Berner, T. Löser, and E. Schöll, Modelling tumor disease and sepsis by networks of adaptively coupled phase oscillators, *Front. Netw. Physiol.* **1**, 730385 (2022).
- [47] R. Berner, J. Sawicki, M. Thiele, T. Löser, and E. Schöll, Critical parameters in dynamic network modeling of sepsis, *Front. Netw. Physiol.* **2**, 904480 (2022).
- [48] R. Berner, S. Yanchuk, and E. Schöll, What adaptive neuronal networks teach us about power grids, *Phys. Rev. E* **103**, 042315 (2021).
- [49] N. T. K. Thanh, N. Maclean, and S. Mahiddine, Mechanisms of nucleation and growth of nanoparticles in solution, *Chem. Rev.* **114**, 7610 (2014).
- [50] L. Schimansky-Geier, C. Zülicke, and E. Schöll, Domain formation due to Ostwald ripening in bistable systems far from equilibrium, *Z. Phys. B* **84**, 433 (1991).
- [51] T. Aoki and T. Aoyagi, Co-Evolution of Phases and Connection Strengths in a Network of Phase Oscillators, *Phys. Rev. Lett.* **102**, 034101 (2009).
- [52] L. Muller, R. Brette, and B. Gutkin, Spike-timing dependent plasticity and feed-forward input oscillations produce precise and invariant spike phase-locking, *Front. Comput. Neurosci.* **5**, 45 (2011).
- [53] J. A. Acebrón, L. L. Bonilla, C. J. Pérez Vicente, F. Ritort, and R. Spigler, The Kuramoto model: A simple paradigm for synchronization phenomena, *Rev. Mod. Phys.* **77**, 137 (2005).
- [54] Note that the choice of  $\hat{\omega}$  is arbitrary as it can be compensated by the rescaling of  $\sigma$ ,  $\epsilon$ , and time  $t$ .
- [55] R. Berner, J. Fialkowski, D. V. Kasatkin, V. I. Nekorkin, S. Yanchuk, and E. Schöll, Hierarchical frequency clusters in adaptive networks of phase oscillators, *Chaos* **29**, 103134 (2019).
- [56] See Supplemental Material at <http://link.aps.org/supplemental/10.1103/PhysRevLett.130.067402> for details on the numerical implementation, the synchronization transition with equiprobable natural frequencies, with multimodal natural frequencies and for other values of  $\beta$ , the hysteretic behavior, the antipodal symmetry of the adaptive network model, the derivation and analysis of the mean-field equations and for details on the clustering behavior during the transition to synchrony.
- [57] For the finite time evaluation in the numerical analysis, we use the threshold  $\langle \dot{\phi}_i \rangle - \langle \dot{\phi}_j \rangle \leq 10^{-3}$ .
- [58] Y. L. Maistrenko, B. Lysyansky, C. Hauptmann, O. Burylko, and P. A. Tass, Multistability in the Kuramoto model with synaptic plasticity, *Phys. Rev. E* **75**, 066207 (2007).
- [59] G. A. Gottwald, Model reduction for networks of coupled oscillators, *Chaos* **25**, 053111 (2015).
- [60] L. D. Smith and G. A. Gottwald, Chaos in networks of coupled oscillators with multimodal natural frequency distributions, *Chaos* **29**, 093127 (2019).
- [61] E. J. Hancock and G. A. Gottwald, Model reduction for Kuramoto models with complex topologies, *Phys. Rev. E* **98**, 012307 (2018).

- [62] L. D. Smith and G. A. Gottwald, Model reduction for the collective dynamics of globally coupled oscillators: From finite networks to the thermodynamic limit, *Chaos* **30**, 093107 (2020).
- [63] Note that the ansatz (3) is only valid for fully connected networks [61] but the numerical results show that this simplification is justified.
- [64] Note that the case of an arbitrary number of clusters can be achieved within the framework of collective coordinates [60,61].
- [65] P. Feketa, A. Schaum, and T. Meurer, Stability of cluster formations in adaptive Kuramoto networks, *IFAC-PapersOnLine* **54**, 14 (2021).
- [66] P. S. Skardal, D. Taylor, and J. G. Restrepo, Complex macroscopic behavior in systems of phase oscillators with adaptive coupling, *Physica (Amsterdam)* **267D**, 27 (2014).
- [67] X. Zhang, S. Boccaletti, S. Guan, and Z. Liu, Explosive Synchronization in Adaptive and Multilayer Networks, *Phys. Rev. Lett.* **114**, 038701 (2015).
- [68] V. Avalos-Gaytán, J. A. Almendral, I. Leyva, F. Battiston, V. Nicosia, V. Latora, and S. Boccaletti, Emergent explosive synchronization in adaptive complex networks, *Phys. Rev. E* **97**, 042301 (2018).
- [69] H. R. Pruppacher and J. D. Klett, *Microphysics of clouds and precipitation*, *Atmospheric and Oceanographic Sciences Library* (Springer, Dordrecht, 2010).
- [70] J. W. Mullin, *Crystallization* (Elsevier, New York, 2001).
- [71] E. Ott and T. M. Antonsen, Low dimensional behavior of large systems of globally coupled oscillators, *Chaos* **18**, 037113 (2008).
- [72] M. A. Gkogkas, C. Kuehn, and C. Xu, Mean field limits of co-evolutionary heterogeneous networks, *arXiv:2202.01742*.
- [73] H. Tanaka, A. J. Lichtenberg, and S. Oishi, First Order Phase Transition Resulting from Finite Inertia in Coupled Oscillator Systems, *Phys. Rev. Lett.* **78**, 2104 (1997).
- [74] P. Ji, T. K. D. M. Peron, P. J. Menck, F. A. Rodrigues, and J. Kurths, Cluster Explosive Synchronization in Complex Networks, *Phys. Rev. Lett.* **110**, 218701 (2013).